ELSEVIER

Inorganica Chimica Acta 229 (1995) 17–25

Inorganica Chimica Acta

Conformational diversity in the solid state structures of $[Rh_2(\mu\text{-}CH_3N(P(OCH_3)_2)_2)_2(CH_3N(P(OCH_3)_2)_2)_2]X_2$ $(X = O_3SCF_3,\ B(C_6H_5)_4)$ ☆

Joel T. Mague

Department of Chemistry, Tulane University, New Orleans, LA 70118, USA

Received 11 January 1994; revised 12 September 1994

Abstract

A significant variation in the conformation of several ligand methoxy groups in $[Rh_2(\mu\text{-}CH_3N(P(OCH_3)_2)_2)_2(CH_3N(P(OCH_3)_2)_2)_2]X_2$ ($X = O_3SCF_3$ (**1**), $B(C_6H_5)_4$ (**2**, **3a**, **3b**)) which results in Rh–Rh separations ranging from 3.2727(5) Å in **1** to 3.0821(39) Å in **3b** within the dinuclear cations is found in the solid state structures of the triflate salt (**1**) and two crystalline modifications of the tetraphenylborate salt (**2**, **3**). This is attributed to variations in the extent of interionic contacts which arise from the different sizes and packing of the anions in the crystal. The looser packing in the tetraphenylborate salts also permits a thermally activated conformational change in the triplet excited state. Complex **2**: $[Rh_2(\mu\text{-}CH_3N(P(OCH_3)_2)_2)_2(CH_3N(P(OCH_3)_2)_2)_2](B(C_6H_5)_4)_2$, monoclinic, $P2_1/n$, $a = 13.899(3)$, $b = 19.986(5)$, $c = 28.089(8)$ Å, $\beta = 90.92(2)°$, $Z = 4$. Complex **3**: $[Rh_2(\mu\text{-}CH_3N(P(OCH_3)_2)_2)_2(CH_3N(P(OCH_3)_2)_2)_2](B(C_6H_5)_4)_2 \cdot 0.64CH_2Cl_2$, monoclinic, $C2/c$, $a = 65.943(12)$, $b = 14.280(3)$, $c = 27.055(6)$ Å, $\beta = 96.41(2)°$, $Z = 12$.

Keywords: Crystal structures; Rhodium complexes; Bidentate ligand complexes; Dinuclear complexes

1. Introduction

The synthesis and chemistry of both homo- and heterometallic, dinuclear complexes is an area of significant continuing interest [1–3] stimulated in part by the proposition that such species may serve to model some aspects of catalysis at multiple metal centers. Among the variety of bridging ligands used to stabilize dinuclear species, some of the more versatile have proved to be the 'short-bite' diphosphines $CH_2(PR_2)_2$ (R = Ph(DPPM), Me(dmpm)) [4–6]. As work with DPPM has developed, it has become increasingly clear that the ligand bulk seriously restricts access to the metal atoms and more emphasis has subsequently been placed on similar complexes with less bulky ligands. While dmpm is clearly an attractive alternative, its high cost and extreme air-sensitivity prompted a search for ligands of similar size and geometry. One such is $MeN(P(OMe)_2)_2$ which is comparatively easy to prepare in large quantities [7] and to handle.

At the time this work was undertaken, the chemistry of this ligand towards the platinum group metals had not been significantly investigated although some interesting dinuclear rhodium complexes of the related ligands $EtN(P(OR)_2)_2$ (R = Me [8], Ph [9]) were known. As reported earlier [10] the reaction of $MeN(P(OMe)_2)_2$ with cationic Rh(I) species not containing carbonyl ligands does not yield the expected 'A-frame' type dinuclear complexes but rather ones containing the 'basket' shaped $[Rh_2(\mu\text{-}MeN(P(OMe)_2)_2)_2(MeN(P(OMe)_2)_2)_2]^{2+}$ cation. The several salts of this cation prepared are intensely red-brown to purple in color which can be attributed to a 'proximity shifted' absorption band [11] in the visible region as the result of the approximately square planar $\{RhP_4\}$ moieties being in a 'face-to-face' orientation. Following determination of the structure of the triflate salt [10], we undertook a study of the electronic absorption spectra of some of these salts and discovered significant differences between the temperature dependencies of the emission spectra of the triflate and the tetraphenylborate salts [12]. This prompted an investigation of the structure of the latter from which it was found that two crystalline

☆ This paper is dedicated to Professor F.A. Cotton on the occasion of his 65th birthday.

SSDI 0020-1693(94)04221-G

modifications could be prepared. We report here on the results of these studies.

2. Experimental

Solutions of $[Rh_2(MeN(P(OMe)_2)_2)_2](BPh_4)_2$, prepared as previously described [10], in acetone/methanol and in dichloromethane/methanol were slowly concentrated in a stream of nitrogen to yield dark, red–violet, columnar crystals of **2** and **3**, respectively. These were mounted in nitrogen-filled, thin-walled glass capillaries and flame-sealed. General procedures for crystal orientation, unit cell determination and the collection of intensity data on the CAD-4 diffractometer have been published [10]. Details specific to this study are given in Table 1. In both instances, the initial monoclinic cells obtained by the CAD-4 software were confirmed by the observation of 2/*m* diffraction symmetry. From the systematic absences observed in the final data sets, the space group for **2** was uniquely determined as $P2_1/n$ while for **3** either *Cc* or *C*2/*c* was possible. That *C*2/*c* was correct was indicated by intensity statistics and this was confirmed by the successful refinement. For **2**, the low temperature during the data collection was maintained by a stream of cold nitrogen from an Enraf-Nonius low temperature attachment. Prior to the data collection for **3**, peak profiles were determined for reflections in representative regions of reciprocal space as a function of scan angle and the size of the detector aperture to determine whether overlap of reflections due to the large size of the *a*-axis might be a problem. The values chosen for these parameters appeared to eliminate this as a general problem but in the final data set, approximately 50 reflections had highly asymmetric backgrounds suggesting possible overlap and these were omitted. The raw intensities were corrected for Lorentz and polarization effects and for absorption based on ψ scans of five reflections with χ near 90°. The intensities of the check reflections showed only statistical fluctuations so no correction for crystal decay was necessary. Equivalent reflections were averaged resulting in agreement factors (on *F*) of 0.02 for each data set. The structures were solved by direct methods (MULTAN [13]) and developed by successive

Table 1
Crystal and intensity collection data for **2** and **3**

	2	**3**
Formula	$C_{68}H_{100}O_{16}P_8N_4B_2Rh_2$	$C_{68}H_{100}O_{16}P_8N_4B_2Rh_2 \cdot 0.64CH_2Cl_2$
Formula weight	1704.92	1759.28
Crystal system	monoclinic	monoclinic
Space group	$P2_1/n$	*C*2/*c*
a (Å)	13.889(3)	65.943(12)
b (Å)	19.986(5)	14.280(3)
c (Å)	28.089(8)	27.055(6)
β (°)	90.92(2)	96.41(2)
V (Å^3)	7796	25318
Z	4	12
D_{calc} (g cm^{-3})	1.45	1.38
Radiation, λ (Å)	Mo Kα, graphite monochromated, 0.71073	
T (K)	135	298
Linear absorption coefficient (cm^{-1})	6.4	6.2
Transmission factor range	0.92–1.0	0.97–1.0
θ Range (°)	1.5–21.5	1.5–16.0
Scan type	ω–2θ	ω–2θ
Scan width (°)	0.80 + 0.20 tan θ	0.65 − 0.20 tan θ
Scan rate (° min^{-1})	1.5–16.5	1.2–16.5
Attenuation factor	11.84	11.84
p Factor in weight	0.04	0.04
Unique data	8835	6231
Data used in refinement	7026 ($I > 3\sigma(I)$)	4125 ($I > 2\sigma(I)$)
No. variables	451	652
Largest shift/e.s.d. in final cycle	0.01	0.13 [a]
R [b]	0.037	0.093
R_w [c]	0.055	0.126
GOF [d]	1.92	3.95

[a] Excluding disordered atoms.
[b] $R = \Sigma||F_o| - |F_c||/\Sigma|F_o|$.
[c] $R_w = [\Sigma w(||F_o| - |F_c||)^2/\Sigma w(|F_o|)^2]^{1/2}$.
[d] $GOF = [\Sigma w(||F_o| - |F_c||)^2/(N_o - N_v)]^{1/2}$, where N_o and N_v are the number of observations and variables, respectively.

cycles of full-matrix, least-squares refinement followed by $\Delta\rho$ syntheses. The neutral atom scattering factors used include corrections for the real and imaginary components of the effects of anomalous dispersion [14]. The refinement of **2** proceeded uneventfully and in the final stages all hydrogen atoms were visible in a $\Delta\rho$ map. These were included as fixed contributions (C–H = 0.95 Å) with isotropic thermal parameters 30% larger than those of the attached carbon atoms and allowed to ride on those atoms. The final $\Delta\rho$ map was essentially featureless. Final positional parameters are presented in Table 2; see also Section 4.

For **3** it was immediately apparent that one of the two independent cations was disordered about the center of symmetry located at 1/4, 1/4, 1/2. The two orientations adopted by the disordered cation are such that the two rhodium atoms appear to coincide almost exactly while the positions of the phosphorus atoms and seven of the light atoms are well-resolved. The positions of the remainder of the light atoms overlap considerably between the two orientations but reasonable locations could be derived from careful inspection of $\Delta\rho$ maps. Thus in the refinement of the disordered cation, one rhodium atom was included at full occupancy while the remaining atoms were assigned occupancies of 0.5. This assignment was confirmed by the essentially equivalent thermal parameters for the two sets of disordered phosphorus atoms. It proved impossible to refine both sets of overlapping light atoms simultaneously so in the final stages these sets were refined alternately. Following location and refinement of all non-hydrogen atoms of the two cations and the three independent anions a molecule of solvent dichloromethane was located. This appeared from an only partially successful refinement to have an occupancy of ~0.64. Because of the small number of data and the limits of the least-squares program only the metal atoms were refined anisotropically and only 53 of the 60 phenyl hydrogen atoms could be included. These were placed in calculated positions as described earlier and not refined. The final $\Delta\rho$ map showed, in addition to peaks attributable to uncorrected anisotropic thermal motion, hydrogen atoms not able to be included and possible disorder in the solvent molecule, a peak of ~1.8 e $Å^{-3}$ about 1.9 Å from each rhodium atom. We have no ready explanation for these but note that in a subsequent data collection a problem with the setting of the sector wheel in the detector became evident. It is therefore possible that a small systematic error may be present in the data but if so it was not apparent even in a careful inspection of the diffractometer output. While the presence of these unexplained peaks undoubtedly contributes to the rather high value of R, the structural features of chemical interest are satisfactorily established and given the disorder problem, further attempts at refinement do not appear fruitful.

Table 2
Positional parameters for $[Rh_2(MeN(P(OMe)_2)_2)_4](BPh_4)_2$ (2)

Atom	x	y	z	B_{eq} (Å²)
Rh(1)	0.64784(3)	0.21141(2)	0.69596(1)	1.096(8)
Rh(2)	0.81726(3)	0.24726(2)	0.62538(1)	1.065(8)
P(1)	0.67149(9)	0.27518(7)	0.76216(5)	1.46(3)
P(2)	0.65818(9)	0.14651(7)	0.76237(5)	1.50(3)
P(3)	0.59584(9)	0.12967(6)	0.64736(5)	1.30(3)
P(4)	0.59409(9)	0.29342(6)	0.64643(5)	1.23(3)
P(5)	0.71463(9)	0.27616(7)	0.56616(5)	1.26(3)
P(6)	0.89230(9)	0.34742(6)	0.62646(5)	1.38(3)
P(7)	0.78696(9)	0.13739(6)	0.61528(5)	1.25(3)
P(8)	0.94094(9)	0.24702(6)	0.67936(5)	1.34(3)
N(1)	0.6744(3)	0.1083(2)	0.6054(1)	1.24(7)*
N(2)	0.6040(3)	0.2890(2)	0.5864(1)	1.13(7)*
N(3)	0.6822(3)	0.2101(2)	0.7997(2)	1.59(8)*
N(4)	0.9732(3)	0.3261(2)	0.6690(1)	1.44(7)*
C(1)	0.6484(4)	0.0657(3)	0.5634(2)	2.3(1)*
C(2)	0.5201(4)	0.3014(3)	0.5537(2)	1.9(1)*
C(3)	0.6957(4)	0.2071(3)	0.8520(2)	2.7(1)*
C(4)	1.0565(4)	0.3654(3)	0.6861(2)	2.2(1)*
O(11)	0.7594(2)	0.3205(2)	0.7798(1)	1.63(6)*
O(12)	0.5800(2)	0.3189(2)	0.7751(1)	1.79(6)*
O(21)	0.7302(2)	0.0879(2)	0.7767(1)	1.94(6)*
O(22)	0.5674(2)	0.1083(2)	0.7828(1)	1.72(6)*
O(31)	0.5742(2)	0.0651(2)	0.6791(1)	1.65(6)*
O(32)	0.5025(2)	0.1375(2)	0.6142(1)	1.68(6)*
O(41)	0.6364(2)	0.3647(2)	0.6624(1)	1.48(6)*
O(42)	0.4803(2)	0.3040(2)	0.6453(1)	1.57(6)*
O(51)	0.7523(2)	0.3431(2)	0.5415(1)	1.66(6)*
O(52)	0.6901(2)	0.2280(2)	0.5221(1)	1.51(6)*
O(61)	0.8440(2)	0.4149(2)	0.6426(1)	1.85(7)*
O(62)	0.9531(2)	0.3729(2)	0.5824(1)	1.64(6)*
O(71)	0.8316(2)	0.0920(2)	0.6574(1)	1.52(6)*
O(72)	0.8331(2)	0.1066(2)	0.5683(1)	1.63(6)*
O(81)	0.9159(2)	0.2375(2)	0.7339(1)	1.77(6)*
O(82)	0.0425(2)	0.2108(2)	0.6734(1)	1.60(6)*
C(11)	0.7761(4)	0.3833(3)	0.7552(2)	2.6(1)*
C(12)	0.5613(4)	0.3437(3)	0.8228(2)	3.1(1)*
C(21)	0.8330(4)	0.0985(3)	0.7751(2)	2.3(1)*
C(22)	0.4729(4)	0.1385(3)	0.7785(2)	2.7(1)*
C(31)	0.5362(4)	0.0034(3)	0.6597(2)	2.7(1)*
C(32)	0.4086(4)	0.1455(3)	0.6363(2)	2.4(1)*
C(41)	0.6094(4)	0.4253(3)	0.6376(2)	2.3(1)*
C(42)	0.4302(4)	0.3202(3)	0.6892(2)	2.1(1)*
C(51)	0.7036(4)	0.3773(3)	0.5031(2)	2.4(1)*
C(52)	0.7661(4)	0.2137(3)	0.4887(2)	2.1(1)*
C(61)	0.8804(5)	0.4811(3)	0.6327(3)	4.1(1)*
C(62)	0.9956(4)	0.3245(3)	0.5506(2)	2.0(1)*
C(71)	0.8216(4)	0.0202(3)	0.6559(2)	2.5(1)*
C(72)	0.9365(4)	0.1158(3)	0.5611(2)	2.2(1)*
C(81)	0.9802(4)	0.2561(3)	0.7730(2)	2.5(1)*
C(82)	1.0537(4)	0.1416(3)	0.6871(2)	2.3(1)*
B(1)	0.7465(4)	0.3520(3)	1.0004(2)	1.5(1)*
C(111)	0.6398(3)	0.3592(2)	0.9741(2)	1.09(8)*
C(112)	0.6015(3)	0.4212(3)	0.9605(2)	1.67(9)*
C(113)	0.5126(3)	0.4277(3)	0.9379(2)	1.7(1)*
C(114)	0.4575(3)	0.3717(3)	0.9274(2)	1.8(1)*
C(115)	0.4936(3)	0.3095(3)	0.9397(2)	1.71(9)*
C(116)	0.5827(3)	0.3039(2)	0.9624(2)	1.38(9)*
C(121)	0.7678(3)	0.4192(2)	1.0331(2)	1.34(9)*
C(122)	0.7004(4)	0.4417(3)	1.0665(2)	1.8(1)*
C(123)	0.7167(4)	0.4955(3)	1.0961(2)	2.3(1)*

(continued)

Table 2 (*continued*)

Atom	x	y	z	B_{eq} (Å^2)
C(124)	0.8019(4)	0.5318(3)	1.0923(2)	2.5(1)*
C(125)	0.8684(4)	0.5131(3)	1.0592(2)	2.0(1)*
C(126)	0.8513(3)	0.4578(2)	1.0301(2)	1.48(9)*
C(131)	0.8306(3)	0.3446(2)	0.9603(2)	1.27(9)*
C(132)	0.8168(3)	0.3532(2)	0.9117(2)	1.37(9)*
C(133)	0.8904(4)	0.3466(3)	0.8784(2)	1.9(1)*
C(134)	0.9833(4)	0.3323(3)	0.8938(2)	1.79(9)*
C(135)	1.0005(3)	0.3241(3)	0.9419(2)	1.66(9)*
C(136)	0.9261(3)	0.3301(3)	0.9745(2)	1.57(9)*
C(141)	0.7465(3)	0.2839(2)	1.0338(2)	1.27(9)*
C(142)	0.7178(3)	0.2823(2)	1.0809(2)	1.54(9)*
C(143)	0.7182(4)	0.2251(3)	1.1083(2)	2.0(1)*
C(144)	0.7466(4)	0.1648(3)	1.0890(2)	1.9(1)*
C(145)	0.7725(4)	0.1634(3)	1.0416(2)	2.0(1)*
C(146)	0.7725(4)	0.2216(3)	1.0146(2)	1.7(1)*
B(2)	0.1996(4)	0.0978(3)	0.8520(2)	1.6(1)*
C(211)	0.2146(3)	0.1689(2)	0.8230(2)	1.23(9)*
C(212)	0.2160(3)	0.2309(3)	0.8461(2)	1.53(9)*
C(213)	0.2359(4)	0.2902(3)	0.8223(2)	2.0(1)*
C(214)	0.2531(4)	0.2899(3)	0.7739(2)	1.9(1)*
C(215)	0.2517(4)	0.2300(3)	0.7495(2)	1.70(9)*
C(216)	0.2379(3)	0.1705(2)	0.7744(2)	1.22(9)*
C(221)	0.2952(3)	0.9828(2)	0.8852(2)	1.51(9)*
C(222)	0.3647(3)	0.1303(3)	0.8980(2)	1.7(1)*
C(223)	0.4423(4)	0.1162(3)	0.9282(2)	2.1(1)*
C(224)	0.4541(4)	0.0531(3)	0.9471(2)	2.5(1)*
C(225)	0.3889(4)	0.0039(3)	0.9349(2)	2.9(1)*
C(226)	0.3118(4)	0.0189(3)	0.9038(2)	2.2(1)*
C(231)	0.1841(3)	0.0396(2)	0.8114(2)	1.55(9)*
C(232)	0.2602(4)	0.0070(3)	0.7890(2)	1.9(1)*
C(233)	0.2484(4)	−0.0320(3)	0.7494(2)	2.2(1)*
C(234)	0.1561(4)	−0.0411(3)	0.7289(2)	2.4(1)*
C(235)	0.0790(4)	−0.0122(3)	0.7510(2)	2.0(1)*
C(236)	0.0924(3)	0.0274(3)	0.7911(2)	1.73(9)*
C(241)	0.1012(3)	0.0985(2)	0.8851(2)	1.47(9)*
C(242)	0.0356(4)	0.1516(3)	0.8866(2)	2.0(1)*
C(243)	−0.0488(4)	0.1497(3)	0.9124(2)	3.2(1)*
C(244)	−0.0702(4)	0.0928(3)	0.9386(2)	3.2(1)*
C(245)	−0.0094(4)	0.0399(3)	0.9384(2)	3.0(1)*
C(246)	0.0764(4)	0.0432(3)	0.9124(2)	2.2(1)*

Starred atoms were refined isotropically. Anisotropically refined atoms are given in the form of the isotropic equivalent displacement parameter defined as: $B_{eq} = (\delta\pi/3)\Sigma_i\Sigma_j U_{ij} a_i^* a_j^* \mathbf{a}_i \cdot \mathbf{a}_j$.

Final positional parameters are presented in Table 3; see also Section 4. All computations were performed on a PDP 11/73 computer with the Enraf-Nonius SDP program package [15].

3. Results and discussion

The structures of both **2** and **3** consist of discrete dimeric cations interspersed with tetraphenylborate anions with no unusually short interionic contacts. As noted above, **3** contains two independent cations, **3a** and **3b**, one of which (**3b**) is disordered about a center of symmetry. A perspective view of the cation in **2** is

Table 3
Positional parameters for $[Rh_2(MeN(P(OMe)_2)_2)_4](BPh_4)_2 \cdot 0.64CH_2Cl_2$ (**3**)

Atom	x	y	z	B_{eq} (Å^2)
Rh(1)	0.41345(4)	0.2026(2)	0.38612(9)	3.00(6)
Rh(2)	0.41828(4)	0.3323(2)	0.29408(9)	3.34(7)
P(1)	0.4409(1)	0.2430(7)	0.4395(3)	4.2(2)*
P(2)	0.4350(1)	0.0802(6)	0.4027(3)	3.6(2)*
P(3)	0.3872(1)	0.1281(6)	0.3420(3)	3.7(2)*
P(4)	0.3948(1)	0.3292(6)	0.3998(3)	3.1(2)*
P(5)	0.3884(1)	0.4062(6)	0.3021(3)	3.7(2)*
P(6)	0.4392(1)	0.4563(7)	0.3074(3)	4.5(2)*
P(7)	0.4024(1)	0.2060(6)	0.2582(3)	3.3(2)*
P(8)	0.4507(1)	0.2892(7)	0.2862(3)	4.2(2)*
N(1)	0.3823(3)	0.160(1)	0.2812(7)	2.6(5)*
N(2)	0.3780(3)	0.375(2)	0.3538(8)	3.4(6)*
N(3)	0.4522(3)	0.137(2)	0.4429(8)	3.2(6)*
N(4)	0.4607(4)	0.396(2)	0.2995(9)	5.8(7)*
C(1)	0.3619(4)	0.146(2)	0.249(1)	4.5(8)*
C(2)	0.3552(5)	0.384(2)	0.358(1)	6(1)*
C(3)	0.4705(5)	0.103(2)	0.475(1)	5.4(9)*
C(4)	0.4815(5)	0.437(3)	0.296(1)	7(1)*
O(11)	0.4577(3)	0.320(2)	0.4221(8)	7.3(6)*
O(12)	0.4400(3)	0.276(1)	0.4980(7)	5.7(6)*
O(21)	0.4500(3)	0.028(1)	0.3695(7)	5.8(6)*
O(22)	0.4273(3)	−0.009(1)	0.4313(7)	4.9(5)*
O(31)	0.3898(3)	0.017(1)	0.3445(7)	4.7(5)*
O(32)	0.3647(3)	0.140(1)	0.3581(7)	5.0(5)*
O(41)	0.4078(3)	0.412(1)	0.4219(7)	4.0(5)*
O(42)	0.3783(3)	0.314(1)	0.4381(7)	4.6(5)*
O(51)	0.3927(3)	0.519(1)	0.3039(7)	5.8(6)*
O(52)	0.3690(3)	0.394(1)	0.2628(7)	4.8(5)*
O(61)	0.4470(3)	0.506(2)	0.3578(8)	7.0(6)*
O(62)	0.4374(3)	0.545(2)	0.2699(7)	6.2(6)*
O(71)	0.4179(3)	0.121(1)	0.2512(7)	5.0(5)*
O(72)	0.3905(3)	0.223(1)	0.2027(1)	4.6(5)*
O(81)	0.4600(3)	0.216(1)	0.3231(7)	5.7(6)*
O(82)	0.4609(3)	0.268(2)	0.2358(8)	6.4(6)*
C(11)	0.4715(6)	0.382(3)	0.453(1)	9(1)*
C(12)	0.4373(5)	0.219(3)	0.538(1)	8(1)*
C(21)	0.4420(5)	−0.045(3)	0.336(1)	7(1)*
C(22)	0.4119(5)	−0.003(2)	0.466(1)	4.8(8)*
C(31)	0.3739(5)	−0.050(2)	0.322(1)	5.9(9)*
C(32)	0.3612(5)	0.110(2)	0.410(1)	5.0(8)*
C(41)	0.3987(5)	0.498(2)	0.442(1)	4.8(8)*
C(42)	0.3857(5)	0.285(2)	0.489(1)	5.8(9)*
C(51)	0.3757(5)	0.586(3)	0.311(1)	7(1)*
C(52)	0.3698(4)	0.431(2)	0.211(1)	4.3(8)*
C(61)	0.4413(6)	0.597(3)	0.371(2)	10(1)*
C(62)	0.4265(5)	0.539(2)	0.219(1)	5.2(9)*
C(71)	0.4101(5)	0.032(2)	0.223(1)	6.1(9)*
C(72)	0.4028(5)	0.260(2)	0.165(1)	5.4(9)*
C(81)	0.4818(6)	0.204(3)	0.335(1)	8(1)*
C(82)	0.4605(5)	0.178(3)	0.216(1)	8(1)*
Rh(3)	0.25863(4)	0.3488(2)	0.4930(1)	4.30(7)
P(1A)	0.2368(3)	0.439(1)	0.5287(7)	4.7(5)*
P(2A)	0.2756(3)	0.418(1)	0.5564(6)	4.4(5)*
P(3A)	0.2847(3)	0.294(1)	0.4538(6)	4.4(5)*
P(4A)	0.2369(3)	0.336(1)	0.4168(7)	4.9(5)*
P(5A)	0.2661(3)	0.364(1)	0.5815(6)	3.9(4)*
P(6A)	0.2912(3)	0.370(1)	0.4787(7)	5.7(5)*
P(7A)	0.2245(3)	0.367(1)	0.4947(6)	3.4(4)*
P(8A)	0.2604(3)	0.343(1)	0.4158(6)	4.5(5)*

(*continued*)

Table 3 (*continued*)

Atom	x	y	z	B_{eq} (Å²)
B(1)	0.1217(5)	0.281(2)	0.350(1)	3.0(9)*
C(111)	0.1246(4)	0.177(2)	0.378(1)	3.3(7)*
C(112)	0.1448(5)	0.143(2)	0.397(1)	4.9(8)*
C(113)	0.1466(5)	0.048(3)	0.418(1)	7(1)*
C(114)	0.1293(5)	0.000(2)	0.423(1)	5.2(8)*
C(115)	0.1107(5)	0.034(2)	0.407(1)	4.9(8)*
C(116)	0.1082(4)	0.122(2)	0.384(1)	4.0(8)*
C(121)	0.1417(4)	0.300(2)	0.317(1)	3.6(7)*
C(122)	1.1505(5)	0.224(2)	0.292(1)	5.4(9)*
C(123)	0.1665(5)	0.239(2)	0.261(1)	5.2(9)*
C(124)	0.1745(5)	0.330(2)	0.255(1)	5.1(8)*
C(125)	0.1670(4)	0.400(2)	0.280(1)	4.0(8)*
C(126)	0.1513(4)	0.387(2)	0.310(1)	3.4(7)*
C(131)	0.1251(4)	0.364(2)	0.396(1)	3.3(7)*
C(132)	0.1415(5)	0.361(2)	0.435(1)	4.7(8)*
C(133)	0.1451(5)	0.431(2)	0.470(1)	5.2(8)*
C(134)	0.1324(4)	0.508(2)	0.467(1)	4.4(8)*
C(135)	0.1162(5)	0.514(2)	0.430(1)	5.7(9)*
C(136)	0.1125(5)	0.442(2)	0.393(1)	5.6(9)*
C(141)	0.1013(4)	0.291(2)	0.3181(9)	2.3(7)*
C(142)	0.0832(4)	0.296(2)	0.338(1)	3.6(7)*
C(143)	0.0657(4)	0.300(2)	0.309(1)	3.9(8)*
C(144)	0.0651(5)	0.288(2)	0.259(1)	5.1(8)*
C(145)	0.0823(4)	0.279(2)	0.239(1)	3.2(7)*
C(146)	0.1000(4)	0.283(2)	0.268(1)	3.5(7)*
B(2)	0.2894(5)	0.248(3)	0.194(1)	3.5(9)*
C(211)	0.2926(4)	0.354(2)	0.2233(9)	2.5(7)*
C(212)	0.2757(4)	0.408(2)	0.2330(9)	2.3(7)*
C(213)	0.2790(4)	0.494(2)	0.257(1)	3.1(7)*
C(214)	0.2991(4)	0.527(2)	0.271(1)	4.1(8)*
C(215)	0.3152(4)	0.478(2)	0.262(1)	4.3(8)*
C(216)	0.3125(4)	0.390(2)	0.239(1)	3.5(7)*
C(221)	0.3079(4)	0.232(2)	0.158(1)	3.4(7)*
C(222)	0.3155(5)	0.307(2)	0.131(1)	5.6(9)*
C(223)	0.3297(5)	0.291(3)	0.100(1)	7(1)*
C(224)	0.3391(5)	0.203(2)	0.097(1)	6(1)*
C(225)	0.3320(5)	0.129(2)	0.122(1)	6(1)*
C(226)	0.3171(4)	0.145(2)	0.152(1)	4.4(8)*
C(231)	0.2920(4)	0.168(2)	0.2395(9)	2.8(7)*
C(232)	0.2797(5)	0.090(2)	0.239(1)	5.2(9)*
C(233)	0.2827(5)	0.016(2)	0.273(1)	6.2(9)*
C(234)	0.2999(5)	0.020(2)	0.309(1)	4.7(8)*
C(235)	0.3125(5)	0.097(2)	0.310(1)	5.5(9)*
C(236)	0.3087(4)	0.169(2)	0.276(1)	3.8(7)*
C(241)	0.2681(4)	0.238(2)	0.162(1)	2.9(7)*
C(242)	0.2493(4)	0.235(2)	0.184(1)	4.0(8)*
C(243)	0.2302(5)	0.235(2)	0.157(1)	5.5(9)*
C(244)	0.2296(5)	0.234(2)	0.107(1)	6.2(9)*
C(245)	0.2461(5)	0.233(2)	0.081(1)	5.5(9)*
C(246)	0.2645(5)	0.238(2)	0.111(1)	5.3(9)*
B(3)	0.4515(5)	0.263(3)	0.023(1)	3.6(9)*
C(311)	0.4556(4)	0.164(2)	0.057(1)	3.3(7)*
C(312)	0.4762(4)	0.129(2)	0.070(1)	3.9(8)*
C(313)	0.4797(5)	0.046(2)	0.098(1)	4.7(8)*
C(314)	0.4638(4)	−0.002(2)	0.113(1)	4.8(8)*
C(315)	0.4441(4)	0.029(2)	0.102(1)	4.2(8)*
C(316)	0.4401(4)	0.109(2)	0.0746(9)	2.8(7)*
C(321)	0.4693(4)	0.269(2)	−0.017(1)	3.5(7)*
C(322)	0.4725(5)	0.191(2)	−0.047(1)	5.6(9)*
C(323)	0.4879(5)	0.196(3)	−0.082(1)	7(1)*
C(324)	0.4983(5)	0.274(3)	−0.083(1)	7(1)*
C(325)	0.4965(5)	0.348(3)	−0.057(1)	7(1)*
C(326)	0.4817(5)	0.347(2)	−0.024(1)	5.1(8)*
C(331)	0.4538(4)	0.355(2)	0.0604(9)	3.0(7)*
C(332)	0.4636(5)	0.355(3)	0.109(1)	7(1)*
C(333)	0.4665(5)	0.437(2)	0.139(1)	6.4(9)*
C(334)	0.4585(5)	0.517(3)	0.117(1)	7(1)*
C(335)	0.4484(5)	0.525(2)	0.072(1)	5.4(9)*
C(336)	0.4461(5)	0.441(2)	0.044(1)	5.1(8)*
C(341)	0.4287(4)	0.262(2)	−0.007(1)	2.7(7)*
C(342)	0.4242(4)	0.241(2)	−0.056(1)	3.5(7)*
C(343)	0.4045(5)	0.234(2)	−0.079(1)	4.6(8)*
C(344)	0.3891(5)	0.253(2)	−0.052(1)	4.7(8)*
C(345)	0.3933(5)	0.276(2)	−0.004(1)	5.5(9)*
C(346)	0.4123(4)	0.280(2)	0.021(1)	3.9(8)*
N(1A)	0.2124(7)	0.316(3)	0.536(2)	3(1)*
N(2A)	0.2618(8)	0.265(4)	0.615(2)	5(1)*
N(3A)	0.2533(7)	0.468(3)	0.572(2)	5(1)*
N(4A)	0.2849(8)	0.367(4)	0.417(2)	6(1)*
C(1A)	0.198(1)	0.367(7)	0.565(3)	11(3)*
C(2A)	0.238(1)	0.236(5)	0.326(2)	6(2)*
C(4A)	0.295(1)	0.407(6)	0.379(3)	11(3)*
O(51A)	0.2883(6)	0.398(3)	0.593(1)	6(1)*
O(52A)	0.2503(6)	0.429(3)	0.608(1)	5(1)*
O(61A)	0.3110(8)	0.316(4)	0.500(2)	11(2)*
O(62A)	0.3017(7)	0.469(3)	0.491(2)	8(1)*
O(71A)	0.2132(6)	0.343(3)	0.442(1)	5(1)*
0(72A)	0.2173(6)	0.475(3)	0.508(1)	4(1)*
O(81A)	0.2567(6)	0.254(3)	0.387(2)	7(1)*
O(82A)	0.2490(6)	0.412(3)	0.376(1)	5(1)*
C(51A)	0.2998(9)	0.420(4)	0.639(2)	3(2)*
C(52A)	0.247(1)	0.527(6)	0.614(3)	9(2)*
C(61A)	0.333(1)	0.295(7)	0.477(4)	13(3)*
C(62A)	0.292(1)	0.551(5)	0.498(3)	8(2)*
C(71A)	0.1943(9)	0.352(4)	0.424(2)	5(2)*
C(72A)	0.224(1)	0.552(5)	0.473(3)	7(2)*
C(81A)	0.258(1)	0.225(5)	0.335(3)	9(2)*
C(82A)	0.242(1)	0.500(7)	0.385(3)	11(3)*
O(22A)	0.2913(6)	0.503(3)	0.553(1)	6(1)*
C(22A)	0.286(1)	0.578(5)	0.519(2)	7(2)*
C(3A)	0.252(1)	0.529(5)	0.614(2)	6(2)*
O(11A)	0.2190(8)	0.394(4)	0.549(2)	10(2)*
O(12A)	0.2284(7)	0.540(3)	0.509(2)	7(1)*
O(21A)	0.2877(6)	0.360(3)	0.600(2)	6(1)*
O(31A)	0.3065(8)	0.329(4)	0.470(2)	11(2)*
O(32A)	0.2848(8)	0.293(4)	0.395(2)	10(2)*
O(41A)	0.2150(6)	0.356(3)	0.427(1)	5(1)*
O(42A)	0.2392(8)	0.410(4)	0.368(2)	9(1)*
C(11A)	0.200(1)	0.402(7)	0.559(3)	15(3)*
C(12A)	0.211(1)	0.570(6)	0.482(3)	11(3)*
C(21A)	0.299(1)	0.388(5)	0.646(2)	6(2)*
C(31A)	0.329(1)	0.338(7)	0.471(3)	12(3)*
C(32A)	0.294(1)	0.351(6)	0.364(3)	11(3)*
C(41A)	0.1971(9)	0.358(5)	0.386(2)	5(2)*
C(42A)	0.255(1)	0.496(6)	0.379(3)	9(2)*
Cl(1)	0.1705(5)	0.344(2)	0.077(1)	23(1)*
Cl(2)	0.1689(5)	0.152(3)	0.097(1)	26(1)*
C(1S)	0.171(1)	0.251(5)	0.123(3)	11(2)*

Starred atoms were refined isotropically. Anisotropically refined atoms are given in the form of the isotropic equivalent displacement parameter defined as: $B_{eq} = (\delta\pi/3)\Sigma_i\Sigma_j U_{ij} a_i^* a_j^* \mathbf{a}_i \cdot \mathbf{a}_j$.

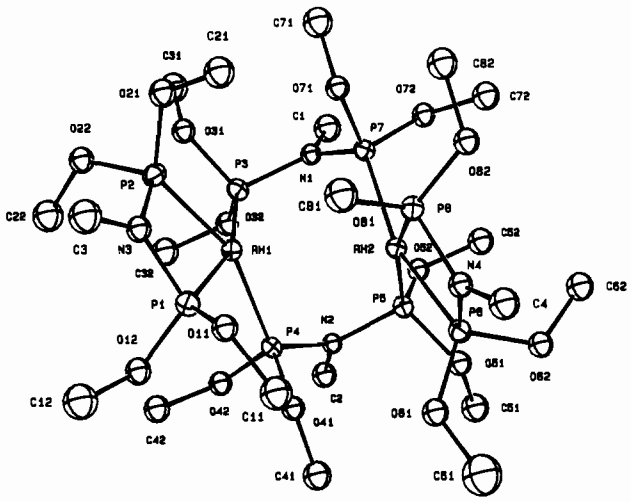

Fig. 1. Perspective view of the cation in **2**. Thermal ellipsoids are drawn at the 50% probability level and hydrogen atoms are omitted for clarity.

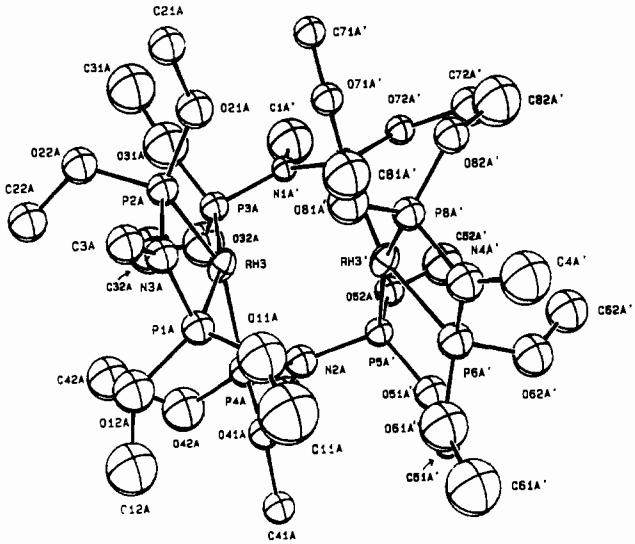

Fig. 3. Perspective view of one orientation of the disordered cation in **3** (**3b**). Thermal ellipsoids are drawn at the 30% probability level.

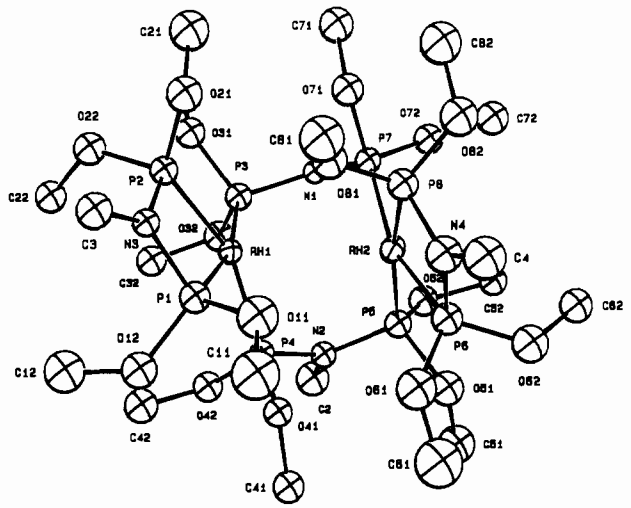

Fig. 2. Perspective view of the ordered cation in **3** (**3a**). Thermal ellipsoids are drawn at the 30% probability level.

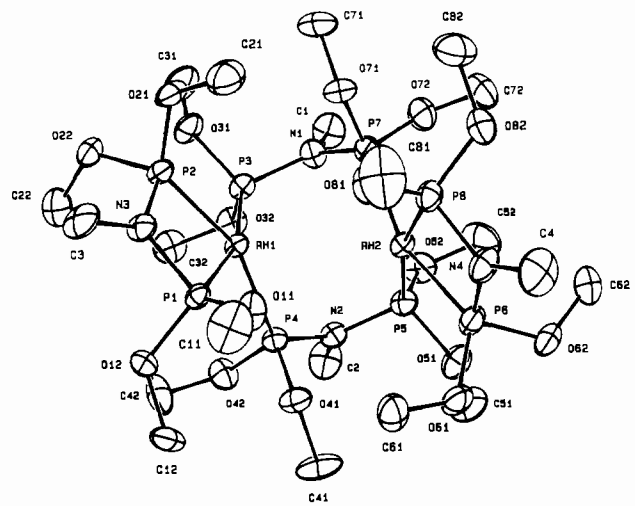

Fig. 4. Perspective view of the cation in **1**. Thermal ellipsoids are drawn at the 30% probability level and hydrogen atoms are omitted for clarity.

given in Fig. 1 while the ordered (**3a**) and disordered (**3b**) cations in **3** are shown in Figs. 2 and 3, respectively. Selected bond distances and interbond angles for all three cations are presented in Tables 4 and 5, respectively. The structure of $[Rh_2(MeN(P(OMe)_2)_2)_4](O_3SCF_3)_2$ (**1**) has been reported previously [10] and a perspective view of the cation is given in Fig. 4 for comparison. In all four cations, the coordination about the metal atoms can be described as severely distorted square planar with the metal atoms displaced towards the center of the cation from the mean planes of the four coordinated phosphorus atoms although it should be noted that those latter atoms deviate significantly from planarity.

As presented in Table 6, the Rh–Rh separations in the cations in solids **1–3** differ considerably. This can be traced to significant differences in the conformations of the methoxy substituents on the chelating ligands (those on the bridging ligands are essentially the same in all three crystals) which appear to be the result of packing considerations. These differences can be seen from the torsional angles listed in Table 7 and most graphically in Figs. 5–7 which highlight the methoxy groups in question. In **1**, which has the longest Rh–Rh separation, the methoxy groups on P(2) and P(6) adopt an unusual 'W' conformation which orients C(21) and C(61) towards the center of the cation (Fig. 5). This conformation is occasioned by close contacts (2.42–2.96 Å) of the methoxy groups {O(21)–C(21)} and {O(61)–C(61)} with two neighboring triflate anions and methoxy groups of two neighboring cations. The resulting positions of C(21) and C(61) generate close contacts with the methoxy groups {O(11)–C(11)} and

Table 4
Selected bond distances (Å) in $[Rh_2(MeN(P(OMe)_2)_2)_4](BPh_4)_2$

	2	3a		3b
Rh(1)–P(1)	2.274(1) [a]	2.260(5)	Rh(3)–P(1A)	2.23(1)
Rh(1)–P(2)	2.275(1)	2.267(5)	Rh(3)–P(2A)	2.18(1)
Rh(1)–P(3)	2.241(1)	2.254(5)	Rh(3)–P(3A)	2.26(1)
Rh(1)–P(4)	2.269(1)	2.238(5)	Rh(3)–P(4A)	2.38(1)
Rh(2)–P(5)	2.249(1)	2.269(5)	Rh(3')–P(5A')	2.40(1)
Rh(2)–P(6)	2.257(1)	2.249(5)	Rh(3')–P(6A')	2.25(1)
Rh(1)–P(7)	2.253(1)	2.249(5)	Rh(3')–P(7A')	2.269(9)
Rh(2)–P(8)	2.273(1)	2.260(5)	Rh(3')–P(8A')	2.11(1)
P(1)–N(3)	1.680(3)	1.69(1)	P(1A)–N(3A)	1.57(3)
P(2)–N(3)	1.679(3)	1.69(1)	P(2A)–N(3A)	1.73(3)
P(3)–N(1)	1.674(3)	1.70(1)	P(3A)–N(1A')	1.61(3)
P(4)–N(2)	1.696(3)	1.70(1)	P(4A)–N(2A)	1.68(5)
P(5)–N(2)	1.666(3)	1.68(1)	P(5A')–N(2A)	1.71(3)
P(6)–N(4)	1.681(3)	1.69(1)	P(6A')–N(4A')	1.67(3)
P(7)–N(1)	1.687(3)	1.67(1)	P(7A')–N(1A')	1.62(2)
P(8)–N(4)	1.670(3)	1.69(1)	P(8A')–N(4A')	1.64(3)

[a] Number in parentheses is e.s.d. in least significant digit.

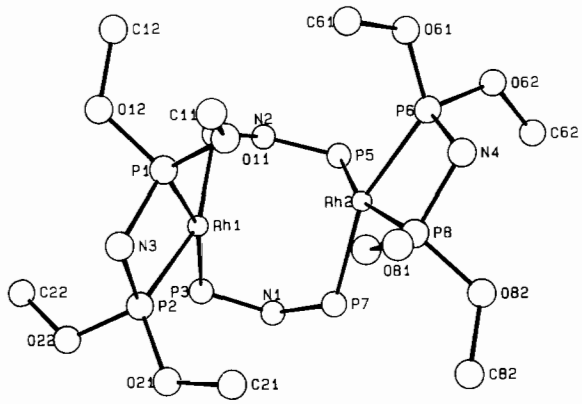

Fig. 5. Perspective view of the cation in **1** showing the conformation of the methoxy groups of the chelating ligands.

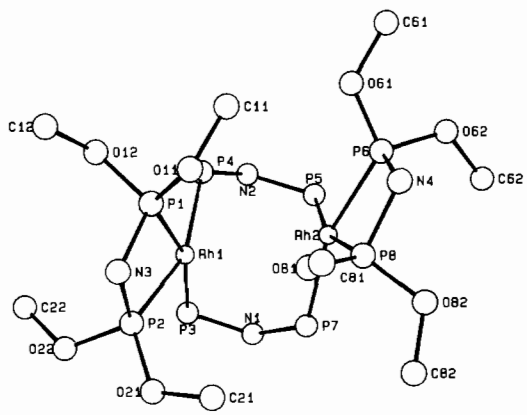

Fig. 6. Perspective view of the cation in **2** showing the conformations of the methoxy groups of the chelating ligands.

{O(81)–C(81)} which constrain these to adopt an 'upright' orientation. These contacts are relieved by a twist of one side of the cation relative to the other but the twist is limited by the approach of {O(11)–C(11)} to {O(81)–C(81)} and a significant opening of the angle

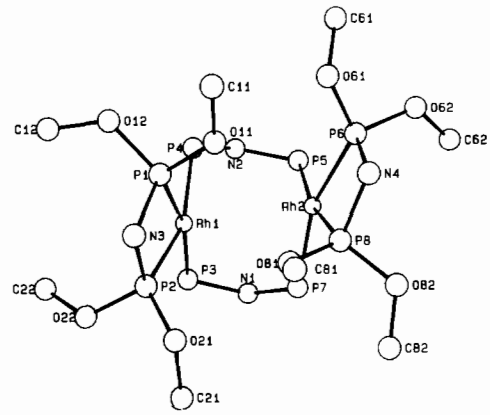

Fig. 7. Perspective view of the cation **3a** showing the conformations of the methoxy groups on the chelating ligands.

between the coordination planes results to give a long metal–metal distance.

In **2**, interionic contacts are fewer and less severe (2.74–2.98 Å). In particular only O(21), O(22) and a hydrogen on C(21) are involved so that only the methoxy groups on P(2) are forced into the 'W' conformation (Fig. 6). Consequently both C(61) and C(11) are oriented away from the center of the cation thereby permitting a greater twist and lessening the steric congestion between the two sides. As a result, the mean coordination planes are less 'opened out' from one another and the metal–metal separation decreases significantly (Table 6).

Cation **3a** is seen (Fig. 7) to have both methoxy groups {O(21), C(21)} and {O(61), C(61)} rotated away from the center of the cation. This less-congested arrangement results from neither of these methoxy groups experiencing interionic contacts of less than 3.3 Å. Consequently, the twist and the 'opening out' of cation **3a** are even less than in **2** and a shorter metal–metal separation ensues.

The situation with **3b** is less clear. Although there appear to be more differences in the orientations of the methoxy groups as compared with **3a**, it is uncertain how real these may be since the disorder made it difficult to accurately position several of the carbon atoms. These differences are not in directions that would affect contacts between the two sides of the cation and thus the twist and opening angles of **3b** are comparable to those of **3a**. This leaves unexplained why the metal–metal separation in **3b** is less than that in **3a** since in the previous examples the decreasing separation was apparently the result of a decrease in the opening angle. It could be argued that we have underestimated the true metal–metal distance in **3b** by the assumption that the two orientations of the disordered rhodium atoms exactly coincide. An indication that they might not is the noticeable elongation of their thermal ellipsoids as compared with those for Rh(1) and Rh(2) in **3a**. However even if one assumes that

Table 5
Selected interbond angles (°) in $[Rh_2(MeN(P(OMe)_2)_2)_4](BPh_4)_2$

	2	3a		3b
P(1)–Rh(1)–P(2)	69.06(4) [a]	68.3(2)	P(1A)–Rh(3)–P(2A)	72.4(4)
P(1)–Rh(1)–P(3)	161.38(4)	166.1(2)	P(1A)–Rh(3)–P(3A)	165.0(4)
P(1)–Rh(1)–P(4)	97.95(4)	95.9(2)	P(1A)–Rh(3)–P(4A)	93.8(4)
P(2)–Rh(1)–P(3)	95.70(4)	99.7(2)	P(2A)–Rh(3)–P(3A)	100.2(4)
P(2)–Rh(1)–P(4)	158.56(4)	159.0(2)	P(2A)–Rh(3)–P(4A)	157.5(4)
P(3)–Rh(1)–P(4)	93.06(4)	93.8(2)	P(3A)–Rh(3)–P(4A)	88.9(4)
P(5)–Rh(2)–P(6)	93.97(4)	98.2(2)	P(5A')–Rh(3')–P(6A')	93.9(4)
P(5)–Rh(2)–P(7)	92.43(4)	92.8(2)	P(5A')–Rh(3')–P(7A')	93.6(3)
P(5)–Rh(2)–P(8)	163.20(4)	168.0(2)	P(5A')–Rh(3')–P(8A')	164.7(4)
P(6)–Rh(2)–P(7)	162.09(4)	161.3(2)	P(6A')–Rh(3')–P(7A')	163.1(4)
P(6)–Rh(2)–P(8)	69.45(3)	70.1(2)	P(6A')–Rh(3')–P(8A')	70.9(4)
P(7)–Rh(2)–P(8)	102.69(4)	98.0(2)	P(7A')–Rh(3')–P(8A')	100.9(4)
Rh(1)–P(1)–N(3)	95.2(1)	97.1(5)	Rh(3)–P(1A)–N(3A)	93.1(4)
Rh(1)–P(2)–N(3)	95.2(1)	96.8(5)	Rh(3)–P(2A)–N(3A)	90(1)
Rh(1)–P(3)–N(1)	114.1(1)	116.1(4)	Rh(3)–P(3A)–N(1A')	110(1)
Rh(1)–P(4)–N(2)	122.7(1)	120.8(5)	Rh(3)–P(4A)–N(2A)	117(1)
Rh(2)–P(5)–N(2)	111.3(1)	113.1(5)	Rh(3')–P(5A')–N(2A)	115(1)
Rh(2)–P(6)–N(4)	95.1(1)	95.2(5)	Rh(3')–P(6A')–N(4A')	92(1)
Rh(2)–P(7)–N(1)	121.8(1)	120.5(4)	Rh(3')–P(7A')–N(1A')	122(1)
Rh(2)–P(8)–N(1)	94.8(1)	94.8(5)	Rh(3)–P(8A')–N(4A')	98(1)
P(3)–N(1)–P(7)	114.1(2)	113.0(7)	P(3A)–N(1A')–P(7A')	119(1)
P(4)–N(2)–P(5)	115.9(2)	114.7(7)	P(4A)–N(2A)–P(5A')	115(1)
P(1)–N(3)–P(2)	100.3(2)	97.8(6)	P(1A)–N(3A)–P(2A)	104(1)
P(6)–N(4)–P(8)	100.7(2)	100.0(8)	P(6A')–N(4A')–P(8A')	100(1)

[a] Number in parentheses is e.s.d. in least significant digit.

Table 6
Comparison of selected features of the $[Rh_2(MeN(P(OMe)_2)_2)_4]^{2+}$ cations

Rh–Rh separation (Å)	3.2727(5)	3.1827(4)	3.1475(19)	3.0821(39)
Dihedral angle between coordination planes [a] (°)	34.84(5)	31.14(4)	27.2(3)	27.8(5)
Twist angle [b] (°)	16.9(2)	22.8(1)	13.7(7)	14(2)

[a] Coordination planes are the weighted, least-squares planes containing P1–P4 and P5–P8, respectively (P1A–P4A and P5A'–P8A' for **3b**).
[b] Taken as the torsional angle N3–Rh1–Rh2–N4 (N3A–Rh3–Rh3'–N4A' for **3b**).

the maximum r.m.s. displacement in the Rh(3) thermal ellipsoid represents the true center of the atom (clearly an overestimate), the metal–metal separation is still ~0.02 Å shorter than in **3a**. It can be noted that Rh(3) in **3b** lies almost 0.1 Å further from the mean plane of its coordinated phosphorus atoms towards the center of the cation than does Rh(1) in **3a** while Rh(3) in **3b** is slightly closer to the corresponding mean plane than is Rh(2) in **3a**. This leads to a shorter metal–metal separation in **3b** but it is still not obvious why this greater distortion occurs. Despite the difficulty in adequately explaining why **3a** and **3b** have different metal–metal separation, it is clear that in both the absence of close contacts with neighboring species in the solid permits orientation of the methoxy groups which minimizes unfavorable contacts between the two sides of the cations.

The results presented here provide a particularly well-documented case of significant variations in the metal–metal separation in a dinuclear complex as the result of packing forces in the solid state although the situation is not unique to the present system. A related finding occurs in the complexes $[Ni_2Cl_2(\mu\text{-}(Et_2PCH_2CH_2)_2PCH_2P(CH_2CH_2)Et_2)_2]X_2$ (X = Cl, BF_4) [16] where the cations in the two salts have different conformations in the solid state which result in an almost 0.2 Å difference in the metal–metal separation between them.

As discussed in a previous paper [12], complexes **1–3** are luminescent in the solid state at low temperature. While the emission spectrum of **1** is invariant over the temperature range 10–80 K, that for **2** shows a decay of the initial 730 nm phosphorescence as the temperature is raised from 10 K until at 80 K it has been completely replaced by one at 780 nm. A similar behavior is noted for **3** although the spectrum is more complex because of the two different conformations of the cation in the solid. An analysis of the luminescence lifetimes led to the conclusion that in **2** and probably in **3** a thermally activated conformational change occurs in the phos-

Table 7
Selected torsion angles (°) in $[Rh_2(MeN(P(OMe)_2)_2)_4)]^{2+}$

	1	2	3a		3b
Rh(1)–P(1)–O(11)–C(11)	102.9(6)	−72.2(4)	−154(2)	Rh(3)–P(1A)–O(11A)–C(11A)	−149(10)
Rh(1)–P(1)–O(12)–C(12)	100.4(6)	−156.3(3)	−76(2)	Rh(3)–P(1A)–O(12A)–C(12A)	99(6)
Rh(1)–P(2)–O(21)–C(21)	−54.4(7)	−53.0(4)	84(2)	Rh(3)–P(2A)–O(21A)–C(21A)	−177(4)
Rh(1)–P(2)–O(22)–C(22)	33.5(7)	33.9(4)	28(2)	Rh(3)–P(2A)–O(22A)–C(22A)	43(4)
Rh(1)–P(3)–O(31)–C(31)	178.6(7)	−177.9(3)	−175(2)	Rh(3)–P(3A)–O(31A)–C(31A)	−180(13)
Rh(1)–P(3)–O(32)–C(32)	68.1(6)	64.5(4)	60(2)	Rh(3)–P(3A)–O(32A)–C(32A)	102(6)
Rh(1)–P(4)–O(41)–C(41)	177.4(7)	177.4(3)	170(2)	Rh(3)–P(4A)–O(41A)–C(41A)	178(3)
Rh(1)–P(4)–O(42)–C(42)	−53.6(8)	−58.4(4)	−60(2)	Rh(3)–P(4A)–O(42A)–C(42A)	−7(5)
Rh(2)–P(5)–O(51)–C(51)	−179.4(7)	178.3(4)	178(2)	Rh(3′)–P(5A′)–O(51A′)–C(51A′)	−178(4)
Rh(2)–P(5)–O(52)–C(52)	63.9(7)	67.3(4)	66(2)	Rh(3′)–P(5A′)–O(52A′)–C(51A′)	77(6)
Rh(2)–P(6)–O(61)–C(61)	−50.2(7)	163.6(4)	111(2)	Rh(3′)–P(6A′)–O(61A′)–C(61A′)	−151(5)
Rh(2)–P(6)–O(62)–C(62)	35.2(8)	26.1(4)	17(2)	Rh(3′)–P(6A′)–O(62A′)–C(62A′)	18(6)
Rh(2)–P(7)–O(71)–C(71)	177.4(6)	178.0(3)	175(2)	Rh(3′)–P(7A′)–O(71A′)–C(71A′)	173(5)
Rh(2)–P(7)–O(72)–C(72)	−56.1(8)	−53.9(3)	−57(2)	Rh(3′)–P(7A′)–O(72A′)–C(72A′)	−58(4)
Rh(2)–P(8)–O(81)–C(81)	155.9(7)	160.5(3)	158(2)	Rh(3′)–P(8A′)–O(81A′)–C(81A′)	174(6)
Rh(2)–P(8)–O(82)–C(82)	97.4(8)	86.9(4)	90(2)	Rh(3′)–P(8A′)–O(82A′)–C(82A′)	−23(6)

phorescing excited state. It was also concluded that the excited state should possess net Rh–Rh bonding and that generation of this interaction provides the driving force for the conformational change. While it is not possible to describe this change in detail, it is clear that in **2** and **3** the reduced interionic contacts in the solid as compared with those in **1** render the cations in the former less constrained by their surroundings and also significantly lessen the steric interactions between the two sides of the cations. All of these factors should make it easier for the photoexcited state in **2** and **3** to adopt a conformation which lessens the Rh–Rh distance, whether this is by twisting of one side relative to the other, a decrease in the dihedral angle between the mean coordination planes, a greater deformation of the coordination geometry about one or both metals or some combination of these.

4. Supplementary material

Additional crystallographic data are available from the author on request.

Acknowledgements

We thank the Chemistry Department of Tulane University for financial support and Dr M. Pontier Johnson for assistance with collection of the low temperature data set.

References

[1] F. Antwi-Nsiah and M. Cowie, *Organometallics, 11* (1992) 3157, and refs. therein.
[2] J.A. Jenkins and M. Cowie, *Organometallics, 11* (1992) 2774, and refs. therein.
[3] J.T. Mague and Z. Lin, *Organometallics, 13* (1994) 3027, and refs. therein.
[4] (a) J.T. Mague and S.H. DeVries, *Inorg. Chem., 21* (1982) 1632; (b) J.T. Mague, *Inorg. Chem., 22* (1983) 45; (c) *Organometallics, 3* (1984) 1860.
[5] (a) B.R. Sutherland and M. Cowie, *Can. J. Chem., 64* (1986) 464; (b) C.P. Kubiak and R. Eisenberg, *Inorg. Chem., 19* (1980) 2726; (c) C.P. Kubiak, C. Woodcock and R. Eisenberg, *Inorg. Chem., 19* (1980) 2733.
[6] J. Wu, P.E. Fanwick and C.P. Kubiak, *Organometallics, 6* (1987) 1805.
[7] G.M. Brown, J.F. Finholt, R.B. King and J.W. Bibber, *Inorg. Chem., 21* (1982) 2139.
[8] R.J. Haines, M. Laing, E. Meintjies and P. Sommerville, *J. Organomet. Chem., 215* (1981) C17.
[9] (a) R.J. Haines, E. Meintjies, M. Laing and P. Sommerville, *J. Organomet. Chem., 216* (1981) C19; (b) J.S. Field, R.J. Haines, E. Meintjies, B. Sigwarth and P.H. Van Rooyen, *J. Organomet. Chem., 268* (1984) C43; (c) R.J. Haines, E. Meintjies and M. Laing, *Inorg. Chim. Acta, 36* (1979) L403.
[10] J.T. Mague and C.L. Lloyd, *Organometallics, 7* (1988) 983.
[11] A.L. Blach and B. Tulyathan, *Inorg. Chem., 16* (1977) 2840.
[12] R.L. Blakley, Y. Yin, C.L. Lloyd, J.T. Mague and G.L. McPherson, *Chem. Phys. Lett., 157* (1989) 398.
[13] P. Main, S.J. Fiske, S.E. Hull, L. Lessinger, G. Germain, J-P. DeClerq and M.M. Woolfson, *MULTAN80*, a system of computer programs for the automatic solution of crystal structures from X-ray diffraction data, University of York, UK, 1980.
[14] (a) D.T. Cromer and J.T. Waber, *International Tables for X-ray Crystallography*, Vol. IV, Kynoch, Birmingham, UK, 1974, Table 2.2B; (b) D.T. Cromer, Table 3.2.1.
[15] *SDP Users Guide*, B.A. Frenz and Associates, Inc., College Station, TX, USA and Enraf-Nonius, Delft, Netherlands, 1985.
[16] S.A. Laneman and G.G. Stanley, *Inorg. Chem., 26* (1987) 1177.